Trajectory Optimization and Resource Allocation for OFDMA UAV Relay Networks

Shuhao Zeng, *Graduate Student Member, IEEE*, Hongliang Zhang, *Member, IEEE*,
Boya Di, *Member, IEEE*, and Lingyang Song, *Fellow, IEEE*

Abstract— In this paper, we consider a single-cell multi-user orthogonal frequency division multiple access (OFDMA) network with one unmanned aerial vehicle (UAV), which works as an amplify-and-forward relay to improve the quality-of-service (QoS) of the user equipments (UEs) in the cell edge. Aiming to improve the throughput while guaranteeing the user fairness, we jointly optimize the communication mode, subchannel allocation, power allocation, and UAV trajectory, which is an NP-hard problem. To design the UAV trajectory and resource allocation efficiently, we first decompose the problem into three subproblems, i.e., mode selection and subchannel allocation, trajectory optimization, and power allocation, and then solve these subproblems iteratively. Simulation results show that the proposed algorithm outperforms the random algorithm and the cellular scheme.

Index Terms— UAV relay, OFDMA network, trajectory optimization, resource allocation.

I. INTRODUCTION

UNMANNED aerial vehicle (UAV) is an emerging facility with a lot of applications, such as environmental monitoring, delivery of goods, etc. Recently, the use of the UAV as relays for providing reliable wireless connections has attracted a lot of attention due to its significant advantages [2]. Benefited from the high mobility, the UAV relay can greatly enhance the link quality by dynamically adjusting its location according to the environment, which is superior to conventional static relays [3]. Besides, the UAV relay is more cost-efficient and can be easily deployed, which makes it more suitable for the emergency cases [4]. In addition, the high altitude of the UAV relay can provide a high probability of line-of-sight communication links, serving as a good solution for QoS-critical scenarios.

In the literature, UAV relaying has been investigated to extend coverage and improve QoS. Existing works on UAV relay networks can be roughly divided into two categories, i.e., distributed UAV relay networks [5], [6] and centralized ones [7], [8]. In [5], the authors evaluated the performance of a UAV ad hoc network, where a swarm of UAVs sense the target area and transmit to the ground station directly or through other UAVs, and each UAV relay determines its routing independently. In [6], sensors on the ground transmit to a cluster head through UAV relays, and all UAVs take part in the UAV deployment optimization by modeling the deployment problem as a local interaction game, which is solved with an online learning approach. Different from the distributed relaying in the UAV ad hoc network, UAV relaying in cellular networks is operated in a centralized manner, which can be more effective. Most works on cellular UAV networks study a simplified network where the UAV relays for only one user [7] or multiple users over a single carrier [8]. In [7], the authors jointly optimized the UAV trajectory and the transmit power of the UAV relay and the mobile device to minimize the outage probability of the network. In [8], the authors considered a wireless sensor network (WSN) with a swarm of UAV relays, where the sensors and the UAVs transmit in a time division multiple access (TDMA) manner, and the UAV transmission schedule was optimized to improve the system energy efficiency. However, none of these works consider the multi-carrier transmission in orthogonal frequency division multiple access (OFDMA) manner.

The resource allocation or trajectory optimization scheme for a UAV enabled network has also been studied, where a UAV is an OFDMA base station (BS) to serve multiple user equipments (UEs) [9]–[11]. However, unlike the UAV BSs which only consider the links between the UAV and the UEs, the UAV relay considered in this paper should take into account both the links from UEs to the UAV and the link from the UAV to the BS, which makes the resource allocation and trajectory optimization different.

In this paper, we study a single-cell OFDMA network consisting of one BS, multiple UEs and one UAV relay. To support the transmission from the UEs to the BS, we consider two communication modes, i.e., cellular and relay modes. Specifically, a UE can transmit to the BS directly or through the UAV relay. To improve the throughput while guaranteeing

the user fairness, new challenges need to be addressed. Due to the multi-carrier transmission, multiple UEs can transmit to the UAV relay simultaneously. Thus, the trajectory of the UAV relay will influence multiple UEs, which makes the trajectory design more difficult. Moreover, the trajectory, communication mode, and resource allocation are coupled. Therefore, it is not trivial to optimize them jointly.

To tackle the above challenges, we formulate a series of joint mode selection, subchannel allocation, trajectory optimization, and power allocation problems, each of which is NP-hard [13]. To solve these problems efficiently, we first decompose each problem into three subproblems, namely the mode selection and subchannel allocation, trajectory optimization, and power allocation problems. Then, we propose a joint mode selection and subchannel allocation, trajectory optimization, and power allocation algorithm (JMS-T-P) to solve these three subproblems iteratively. Specifically, we reformulate the subchannel allocation and mode selection problem as a many-to-one matching problem, which can be solved by the MC-subchannel matching algorithm (MSMA). For the trajectory optimization problem, it is further decomposed into horizontal position optimization and altitude optimization problems, where the trajectory optimization (TO) algorithm is then proposed to solve these two subproblems in a iterative way. Furthermore, the power allocation subproblem is solved by successive convex programming (SCP) technique.

The contributions of this paper are summarized below,
- We consider an OFDMA UAV relay network, where each UE can transmit either in the cellular or the relay mode.
- To improve system performance, we formulate a series of joint mode selection and subchannel allocation, trajectory optimization, and power allocation problems. To solve these problems efficiently, each problem is decoupled into three subproblems, and an efficient JMS-T-P algorithm is proposed afterwards, where the three subproblems are solved iteratively.
- Simulation results show that the proposed JMS-T-P algorithm outperforms the random algorithm and the cellular scheme in terms of sum rate and user fairness.

The rest of this paper is organized as follows. In Section II, the system model for the UAV relay network is introduced. In Section III, we formulate a series of joint trajectory optimization and resource allocation problems, each of which is then decomposed into three subproblems. Then, the JMS-T-P algorithm is proposed to solve these three subproblems iteratively in Section IV, and the convergence and complexity of the JMS-T-P algorithm along with the system performance are discussed in Section V. Afterwards, Section VI evaluates the performance of the JMS-T-P algorithm through numerical simulations. Finally, conclusions are drawn in Section VII.

II. System Model

In this section, the scenario is described first, which is followed by channel models and analysis of the UEs' data rates.

A. Scenario Description

As shown in Fig. 1, we consider an uplink OFDMA cellular network with one BS and N UEs, denoted by
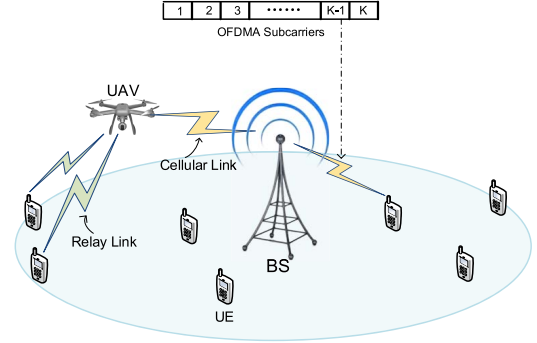

Fig. 1. System model of the OFDMA UAV relaying network.

$\mathcal{N} = \{1, \ldots, N\}$. To improve the QoS of cell-edge users, we introduce one UAV as an amplify-and-forward (AF) relay.

The transmission timeline is divided into T time slots, denoted by $\mathcal{T} = \{1, \ldots, T\}$, where each time slot comprises two phases. To support the transmission from the UEs to the BS, two communication modes are considered in the network:
- **Relay mode**: In the first phase, the UEs transmit to the UAV relay. Then, the UAV relay amplifies the received signal and forwards it to the BS in the second phase [14].
- **Cellular mode**: The UEs transmit to the BS directly.

Here, we use vector $\boldsymbol{\beta} = [\beta_n]_{\mathcal{N}}$ to represent the communication modes of the UEs, where

$$\beta_n = \begin{cases} 1, & \text{UE } n \text{ communicates in the relay mode,} \\ 0, & \text{otherwise.} \end{cases} \quad (1)$$

Following the OFDMA manner, the available spectrum of the network is divided into K subchannels, denoted by $\mathcal{K} = \{1, \ldots, K\}$. To describe the subchannel allocation to the UEs, we define matrix $\boldsymbol{A} = [\alpha_n^k]_{\mathcal{N} \times \mathcal{K}}$, where

$$\alpha_n^k = \begin{cases} 1, & \text{subchannel } k \text{ is assigned to UE } n, \\ 0, & \text{otherwise,} \end{cases} \quad (2)$$

To avoid severe interference, we assume one subchannel is used by at most one UE, i.e.,

$$\sum_{n \in \mathcal{N}} \alpha_n^k \leq 1, k \in \mathcal{K}. \quad (3)$$

It is assumed that the UEs are static and the BS is located at the center of the cell, whose coordinate is given by $\boldsymbol{b} = (0, 0, H_B)$, while the UAV is assumed to be mobile, with its locations in the present and former time slots denoted by $\boldsymbol{q_U} = (x_U, y_U, z_U)$ and $\boldsymbol{q_U^0} = (x_U^0, y_U^0, z_U^0)$, respectively. Define $d_{U,B}$ as the distance between the UAV and the BS. Due to physical limitations, the flying distance of the UAV in the present time slot cannot exceed d_{max}, i.e.,

$$\|\boldsymbol{q_U} - \boldsymbol{q_U^0}\| \leq d_{max}. \quad (4)$$

Besides, we assume that the UAV needs to be higher than the BS to construct a line-of-sight (LoS) link, i.e.,

$$z_U > H_B. \quad (5)$$

To ensure the normal operation of the UAV relay in the following time slots, the energy consumption of the UAV

relay in the present time slot is constrained. According to results in [15], the UAV power consumption mainly comes from flying. Therefore, we have

$$P_f \Delta T \leq E_{max}, \tag{6}$$

where P_f is the flying power of the UAV, ΔT is the length of one time slot, and E_{max} denotes the maximum energy consumption. Here, the maximum energy consumption is determined by deducting the minimum energy consumption required by the following time slots from the remaining battery capacity. To investigate the influence of the energy constraint (6) on the resource allocation and UAV trajectory, we adopt the power consumption model in [16] to describe the flying power of the UAV, i.e.,

$$P_f = P_0(1 + \frac{3v^2}{U_{tip}^2}) + P_i(\sqrt{1 + \frac{v^4}{4v_0^4}} - \frac{v^2}{2v_0^2})^{\frac{1}{2}} + \frac{1}{2}d_0\rho s A v^3, \tag{7}$$

where

$$P_0 = \frac{\delta}{8}\rho s A \Omega^3 R^3, \tag{8}$$

$$P_i = (1 + k)\frac{W^{\frac{3}{2}}}{\sqrt{2\rho A}}, \tag{9}$$

v is the speed of the UAV relay, δ represents profile drag coefficient, Ω is blade angular velocity, R is rotor radius, U_{tip} denotes tip speed of the rotor blade, v_0 is mean rotor induced velocity in hover, d_0 represents fuselage drag ratio, ρ is air density, s denotes rotor solidity, A is rotor disc area, W means aircraft weight, and k represents incremental correction factor to induced power.

Denote the transmit power matrices of the UAV as $\boldsymbol{P_U} = [P_U^k]_{\mathcal{K}}$, where P_U^k is the transmit power of the UAV over subchannel k. For convenience, we use $\alpha_n^k P_n^k$ to represent the transmit power of UE n over subchannel k. Besides, the transmit power matrices of the UEs is defined as $\boldsymbol{P_M} = [P_n^k]_{\mathcal{N} \times \mathcal{K}}$. It is assumed that the transmit powers of each UE and the UAV are constrained, i.e.,

$$\sum_{k \in \mathcal{K}} \alpha_n^k P_n^k \leq P_M^{max}, \tag{10}$$

$$\sum_{k \in \mathcal{K}} P_U^k \leq P_U^{max}, \tag{11}$$

where P_M^{max} and P_U^{max} are the maximum transmit power of the UE and the UAV, respectively.

B. Data Transmission

In this subsection, we present channel models and analyse the data rates for the cellular and relay modes.

1) Cellular Mode: We assume that the channel from UE n to the BS is Rayleigh faded. Therefore, the channel power gain for the channel over subchannel k can be expressed as

$$h_{n,B}^k = (d_{n,B})^{-\alpha}|g_{n,B}^k|^2 \tag{12}$$

where $(d_{n,B})^{-\alpha}$ denotes the pathloss with α being the pathloss coefficient, and $g_{n,B}^k$ represents the Rayleigh small scale fading satisfying $g_{n,B}^k \sim \mathcal{CN}(0,1)$.

Due to the mobility of the UAV relay, inter-subcarrier-interference (ICI) needs to be considered here. Specifically, in the first phase, the link from UE n in the cellular mode to the BS over subchannel k does not suffer from ICI, since both the UEs in the cellular and relay mode are static. However, due to the UAV mobility, the subcarriers allocated to UEs in the relay mode cause ICI to subchannel k of UE n in the second phase. Therefore, the received signal over subchannel k at the BS in the two phases can be rewritten as,

$$Y_B^{(k,1)} = \sqrt{h_{n,B}^k P_n^k}X_n^{(k,1)} + n_B^{(k,1)}, \tag{13}$$

and

$$Y_B^{(k,2)} = \sqrt{h_{n,B}^k P_n^k}X_n^{(k,2)} + I_B^k + n_B^{(k,2)}, \tag{14}$$

respectively, where $X_n^{(k,1)}$ and $X_n^{(k,2)}$ represent data symbols transmitted by UE n over subchannel k in the two phases, respectively, both with unit power, I_B^k is the ICI to subchannel k received at the BS in the second phase, and $n_B^{(k,1)}$ and $n_B^{(k,2)}$ are additive white Gaussian noise (AWGN) in the two phases, respectively, which have equal variance σ^2 and zero mean. Here, we present an approximation for the ICI as shown in Appendix A, from which we can find that *the ICI is relatively weak compared with the desired signal, and thus, it can be regarded as a constant for simplicity*. Based on the received signals in (13) and (14), the average data rate of UE n over subchannel k can be expressed as,

$$R_{n,D}^k = \frac{1}{2}\log_2(1 + \frac{P_n^k h_{n,B}^k}{\sigma^2}) + \frac{1}{2}\log_2(1 + \frac{P_n^k h_{n,B}^k}{\sigma^2 + |I_B^k|^2}). \tag{15}$$

To guarantee the QoS, the received SINR of one link over each occupied subchannel cannot be lower than a predetermined threshold. Therefore, we have,

$$\frac{P_n^k h_{n,B}^k}{\sigma^2} \geq \alpha_n^k(1 - \beta_n)\gamma^{th}, \quad \frac{P_n^k h_{n,B}^k}{\sigma^2 + |I_B^k|^2} \geq \alpha_n^k(1 - \beta_n)\gamma^{th}, \tag{16}$$

where γ^{th} denotes the threshold for a link from a UE to the BS.

2) Relay Mode: For a UE in the relay mode, the communication to the BS consists of a ground-to-air link from the UE to the UAV relay and an air-to-ground link from the UAV relay to the BS. We assume that both channels are Rician faded, i.e., the channel contains pathloss and small scale Rician fading, which will be elaborated on in the following.

First, we introduce the channel from the UAV relay to the BS. According to the air-to-ground propagation pathloss model [17], the LoS and NLoS pathloss from the UAV to the BS over subchannel k can be given by

$$PL_{LoS}^k = L^k(d_{U,B})^2\eta_{LoS},$$
$$PL_{NLoS}^k = L^k(d_{U,B})^2\eta_{NLoS}, \tag{17}$$

respectively, where L^k is the free space pathloss, and η_{LoS} and η_{NLoS} are additional attenuation factors due to the LoS and non-line-of-sight (NLoS) connections. Here, L^k can be expressed as $L^k = (\frac{4\pi f^k}{c})^2$, where f^k is the frequency of

subchannel k in MHz and c is the velocity of light in vacuum. Assume that the antennas on the UAV and the BS are vertically placed. Therefore, the probability of LoS connection is given by

$$PR_{LoS} = \frac{1}{1 + a\exp(-b(\theta - a))}, \quad (18)$$

where a and b are constants depending on the environment, and $\theta = \frac{180}{\pi}\sin^{-1}((z_U - H_B)/d_{U,B})$ is the elevation angle. Based on (17) and (18), the average pathloss of a link can be expressed as

$$PL_{avg}^k = PR_{LoS}PL_{LoS}^k + PR_{NLoS}PL_{NLoS}^k, \quad (19)$$

where $PR_{NLoS} = 1 - PR_{LoS}$ is the probability of the NLoS connection. By combining the pathloss model and small scale fading, the average channel power gain from the UAV relay to the BS over subchannel k can be obtained as

$$h_{U,B}^k = \frac{|g_{U,B}^k|^2}{PL_{avg}^k}, \quad (20)$$

where $g_{U,B}^k$ is the Rician small scale fading.

Note that the channel gain from UE n to the UAV relay $h_{n,U}^k$ is the same as its reverse channel $h_{U,n}^k$ according to the reciprocity of channel [17]. Therefore, we can derive $h_{n,U}^k$ by modeling channel $h_{U,n}^k$ from the UAV relay to UE n, which is similar to the channel model from the UAV to the BS. Specifically, the LoS and NLoS pathloss are given by

$$PL_{LoS}^{n,k} = L^k(d_{n,U})^2\eta_{LoS}, \quad (21)$$
$$PL_{NLoS}^{n,k} = L^k(d_{n,U})^2\eta_{NLoS}, \quad (22)$$

respectively, and the probability of the LoS and NLoS connections can be expressed as

$$PR_{LoS}^n = \frac{1}{1 + a\exp(-b(\theta_n - a))}, \quad (23)$$
$$PR_{NLoS}^n = 1 - PR_{LoS}^n, \quad (24)$$

respectively, where θ_n is the elevation angle from the UAV to UE n. Therefore, the average pathloss is given by

$$PL_{avg}^{n,k} = PR_{LoS}^n PL_{LoS}^{n,k} + PR_{NLoS}^n PL_{NLoS}^{n,k}, \quad (25)$$

based on which we can obtain the average channel power gain from the UAV relay to UE n as

$$h_{U,n}^k = \frac{|g_{U,n}^k|^2}{PL_{avg}^{n,k}}, \quad (26)$$

where $g_{U,n}^k$ represents the Rician small scale fading.

Based on the aforementioned channel models, the received signal at the UAV from UE n over subchannel k is[1]

$$Y_{n,U}^k = \sqrt{P_n^k h_{n,U}^k}X_n^k + n_U^k, \quad (27)$$

where X_n^k is the transmit signal of UE n over subchannel k with unit power, and n_U^k is the AWGN at the UAV relay with

σ^2 as variance and 0 as mean. The amplification coefficient at the UAV relay over subchannel k is given by

$$G^k = \frac{P_U^k}{P_n^k h_{n,U}^k + \sigma^2}. \quad (28)$$

Therefore, the received signal of BS over subchannel k can be expressed as

$$Y_B^k = \sqrt{G^k h_{U,B}^k}Y_{n,U}^k + n_B^k + I_B^k, \quad (29)$$

where n_B^k is the AWGN at the BS over subchannel k, and I_B^k is ICI to subchannel k from the other subchannels allocated to UEs in the relay mode. Here, we can also find that the ICI is weak compared with the desired signal, and thus, we regard it as a constant for simplicity, as shown in Appendix A. According to (27) and (29), the SINR at the UAV relay from UE n and that at the BS from the UAV relay can be calculated by

$$\gamma_{n,U}^k = \frac{P_n^k h_{n,U}^k}{\sigma^2}, \quad (30)$$

and

$$\gamma_{U,B}^k = \frac{P_U^k P_n^k h_{U,B}^k h_{n,U}^k}{\sigma^2\left(P_U^k h_{U,B}^k + (\frac{|I_B^k|^2}{\sigma^2} + 1)P_n^k h_{n,U}^k + (\frac{|I_B^k|^2}{\sigma^2} + 1)\sigma^2\right)}, \quad (31)$$

respectively. Therefore, the data rate of UE n over subchannel k can be given by

$$\begin{aligned}R_{n,R}^k &= \frac{1}{2}\min\{\log_2(1 + \gamma_{n,U}^k), \log_2(1 + \gamma_{U,B}^k)\}\\ &= \frac{1}{2}\log_2(1 + \gamma_{U,B}^k), \quad (32)\end{aligned}$$

where $\frac{1}{2}$ follows because two phases are needed for the transmission from UE n to the BS [12].

Similar to (16), to guarantee the QoS for each link, we have

$$\frac{P_n^k h_{n,U}^k}{\sigma^2} \geq \alpha_n^k \beta_n \gamma_1^{th}, \quad \frac{P_U^k h_{U,B}^k}{\sigma^2 + |I_B^k|^2} \geq \alpha_n^k \beta_n \gamma_2^{th}, \quad (33)$$

where γ_1^{th} denotes the SINR threshold for a link from UEs to the UAV and γ_2^{th} represents that for the link from the UAV to the BS.

Define R_n as the sum rate of UE n, and we have

$$R_n = \beta_n \sum_{k \in \mathcal{K}} \alpha_n^k R_{n,R}^k + (1 - \beta_n) \sum_{k \in \mathcal{K}} \alpha_n^k R_{n,D}^k. \quad (34)$$

III. PROBLEM FORMULATION AND DECOMPOSITION

In this paper, we aim to improve the sum rate over the UEs while achieving the fairness among these UEs. Therefore, we use the proportional fairness algorithm, and the objective function for one time slot is defined as weighted sum rate of the UEs, i.e., $\sum_{n \in \mathcal{N}} w_n R_n$, where weight w_n is set as the inverse of the average rate over previous time slots[2]. Then, the joint mode selection and subchannel allocation, trajectory

---

[1]Since the ICI received at the UAV relay over subchannel k is weak compared with the desired signal, the ICI is neglected here for simplicity.

[2]To ensure that the objective function makes sense even when the UE never transmit to the BS in previous time slots, we add 0.1 to the average rate.

optimization, and power allocation problem for this time slot can be written by

$$\max_{\beta, A, P_U, P_M, q_U} \sum_{n \in \mathcal{N}} w_n R_n, \tag{35a}$$

$$s.t. \ P_n^k, P_U^k \geq 0, \ \sum_{k \in \mathcal{K}} P_U^k \leq P_U^{max}, \tag{35b}$$

$$\sum_{k \in \mathcal{K}} \alpha_n^k P_n^k \leq P_M^{max}, \tag{35c}$$

$$\alpha_n^k, \beta_n \in \{0, 1\}, \ \sum_{n \in \mathcal{N}} \alpha_n^k \leq 1, \tag{35d}$$

$$\|q_U - q_0\| \leq d_{max}, \ z_U > H_B, \tag{35e}$$

$$P_f \Delta T \leq E_{max}, \tag{35f}$$

$$\frac{P_n^k h_{n,B}^k}{\sigma^2} \geq \alpha_n^k (1 - \beta_n) \gamma^{th},$$

$$\frac{P_n^k h_{n,B}^k}{\sigma^2 + |I_B^k|^2} \geq \alpha_n^k (1 - \beta_n) \gamma^{th}, \tag{35g}$$

$$\frac{P_n^k h_{n,U}^k}{\sigma^2} \geq \alpha_n^k \beta_n \gamma_1^{th}, \ \frac{P_U^k h_{U,B}^k}{\sigma^2 + |I_B^k|^2} \geq \alpha_n^k \beta_n \gamma_2^{th}. \tag{35h}$$

Constraint (35b) implies that the transmit power is nonnegative and the transmit power of the UAV is limited. Constraint (35c) corresponds to (10). The minimum altitude and the maximum moving distance of the UAV relay are given in constraint (35e). Constraint (35f) shows that the energy consumption for flying is constrained. Constraints (35g) and (35h) indicate SINR requirements for each communication link, which correspond to (16), and (33).

To solve the NP-hard problem in (35) efficiently, we decompose it into three subproblems, namely mode selection and subchannel allocation, power allocation, and trajectory optimization problems [20], and apply block coordinate descent (BCD) method.[3] Specifically, given transmit power (P_U, P_M) and UAV location q_U, the mode selection and subchannel allocation problem is given by

$$\max_{\beta, A} \sum_{n \in \mathcal{N}} w_n R_n$$
$$s.t. \ (35c), (35d), (35g), \text{ and } (35h). \tag{36}$$

Given transmit power (P_U, P_M), communication modes β and subchannel allocation A, the location of UAV q_U can be optimized by solving the following problem:

$$\max_{q_U} \sum_{n \in \mathcal{N}} w_n R_n$$
$$s.t. \ (35e), (35f), \text{ and } (35h). \tag{37}$$

Given location q_U, subchannel allocation A and communication modes β, the power allocation problem is given by

$$\max_{P_U, P_M} \sum_{n \in \mathcal{N}} w_n R_n$$
$$s.t. \ (35b), (35c), (35g), \text{ and } (35h). \tag{38}$$

[3]Due to the non-convexity of the original problem, the BCD method will converge to a suboptimal solution.

IV. JOINT MODE SELECTION AND SUBCHANNEL ALLOCATION, TRAJECTORY OPTIMIZATION, AND POWER ALLOCATION ALGORITHM DESIGN

In this section, the JMS-T-P algorithm is proposed to solve the subproblems formulated in (36)-(38) iteratively.

A. Mode Selection and Subchannel Allocation

To develop a low complexity algorithm for problem (36), we reformulate the subchannel allocation and mode selection as a matching game. Specifically, define $\mathcal{P}$ as the set of UE-communication mode (MC) pairs, i.e., $\mathcal{P} = \{(n, \beta) | n \in \mathcal{N}, \beta \in \{0, 1\}\}$. We consider the set $\mathcal{P}$ and the set of subchannels $\mathcal{K}$ as two disjoint sets of selfish and rational players aiming to maximize their own benefits, where the pair $(n, 0)$ is considered to be matched with the subchannel k if UE n transmits in the cellular mode with subchannel k. Due to constraint (35d), one subchannel can be matched with at most one MC pair. However, one MC pair can be matched with any number of subchannels. Therefore, the matching game is of the many-to-one type. In addition, since each UE can transmit either in the cellular or the relay mode, no subchannels will be matched with $(n, 1 - \beta)$ if (n, β) is matched with certain subchannels. It is assumed that each player has *preferences* over the players in the other set, and the preferences are determined by the utility of the players, which will be described in the following. Suppose that subchannel k is matched with MC pair (n, β). Then, the utility of subchannel k over MC pair (n, β) is given by

$$U_S^{(n,\beta),k} = w_n \Big(\beta R_{n,R}^k + (1 - \beta) R_{n,D}^k \Big). \tag{39}$$

Similarly, use $\mathcal{K}_0$ to represent the set of subchannels assigned to UE n. Therefore, the utility of the MC pair (n, β) over $\mathcal{K}_0$, i.e., $U_M^{(n,\beta),\mathcal{K}_0}$, is given by

$$U_M^{(n,\beta),\mathcal{K}_0} = \sum_{k \in \mathcal{K}_0} w_n \Big(\beta R_{n,R}^{k,t} + (1 - \beta) R_{n,D}^{k,t} \Big) \tag{40}$$

Then, based on the utility of the players, the preferences of subchannel k, which is denoted by $\succ_k$, can be given below.

Definition 1: For two different MC pairs (n_1, β_1) and (n_2, β_2), and two matchings (Ψ_1, Ψ_2) where $(n_1, \beta_1) = \Psi_1(k)$ and $(n_2, \beta_2) = \Psi_2(k)$:

$$\Big((n_1, \beta_1), \Psi_1 \Big) \succ_k \Big((n_2, \beta_2), \Psi_2 \Big) \Leftrightarrow U_S^{(n_1,\beta_1),k} > U_S^{(n_2,\beta_2),k}. \tag{41}$$

The definition indicates that subchannel k prefers (n_1, β_1) in Ψ_1 to (n_2, β_2) in Ψ_2 when the utility it obtains from the MC pair (n_1, β_1) is larger than that from (n_2, β_2). Similarly, we can define preference $\succ_{(n,\beta)}$ of for the MC pair (n, β) over subsets of subchannels, which is neglected here due to the space limit.

Remark 1: The formulated matching game has externalities.

Proof: Consider the MC pairs $(n, 0)$ and $(n, 1)$. If the pair $(n, 0)$ is matched with some subchannels, $(n, 1)$ will not be matched with any subchannel since UE n cannot transmit in both the cellular and relay modes. Therefore, the matching of

the pair $(n, 0)$ has mutual influence on that of the pair $(n, 1)$, which indicates that the formulated game has externalities. □

Note that under traditional definition of stable matching such as that in [23], the stable matching may not exist for a many-to-one matching game with externalities. Besides, it is computationally hard to find a stable matching if it exists [24]. Therefore, to solve the formulated matching game, we introduce the notion of pairwise stable matching, and then design a MC-subchannel matching algorithm (MSMA) to find one such matching, which will be elaborated on in the following.

Before introducing pairwise stability, we first define swap matching. Specifically, given a matching Ψ, the swap matching $\Psi_{k_1}^{k_2}$ is generated from Ψ via exchanging the matches of subchannels k_1 and k_2 while keeping all other subchannels' matches the same. It is worthwhile noting that a swap operation may not be approved, due to the interests of the players involved in the swap operation and the constraints of problem (36). In the Definition 2, we provide the conditions under which a swap operation will be approved.

Definition 2: Given a matching Ψ and a subchannel pair (k_1, k_2). The swap matching $\Psi_{k_1}^{k_2}$ is approved, and (k_1, k_2) is called a swap-blocking pair under Ψ if

- $\forall v \in \{k_1, k_2, \Psi(k_1), \Psi(k_2)\}, (\Psi_{k_1}^{k_2}(v), \Psi_{k_1}^{k_2}) \succeq_v (\Psi(v), \Psi),$
- $\exists v \in \{\Psi(k_1), \Psi(k_2)\}, (\Psi_{k_1}^{k_2}(v), \Psi_{k_1}^{k_2}) \succ_v (\Psi(v), \Psi),$
- *The constraint of problem (36) hold for $\Psi_{k_1}^{k_2}$.*

The first item in Definition 2 indicates that the utilities of subchannels $\{k_1, k_2\}$ and MC pairs $\{\Psi(k_1), \Psi(k_2)\}$ do not decease after the exchange. The second item means at least one MC pair in $\{\Psi(k_1), \Psi(k_2)\}$ obtains a larger utility after the exchange. The last item states that the transmit power and SNR constraints of problem (36) are satisfied after the exchange. Based on the definition of swap-blocking pair, we say a matching Ψ is pairwise stable if it is not blocked by any swap-blocking pair under Ψ.

To find a pairwise stable matching, we propose algorithm MSMA. First, we present the following lemma on the relationship between the subchannel allocation and the communication mode, which will be utilized in the MSMA algorithm.

Lemma 1: Suppose that the subchannel allocation $\boldsymbol{A}^*$ and the communication mode $\boldsymbol{\beta}^*$ are optimal, and

$$\frac{P_n^k h_{n,B}^k}{\sigma^2 + |I_B^k|^2} \geq (\alpha_n^k)^* \gamma^{th}, \forall k \tag{42}$$

$$\frac{P_n^k h_{n,U}^k}{\sigma^2} \geq (\alpha_n^k)^* \gamma_1^{th}, \quad \frac{P_U^k h_{U,B}^k}{\sigma^2 + |I_B^k|^2} \geq (\alpha_n^k)^* \gamma_2^{th}, \forall k. \tag{43}$$

Then, we have

1) $(\beta_n)^* = 1$, if $\sum_{k \in \mathcal{K}} (\alpha_n^k)^* R_{n,R}^k > \sum_{k \in \mathcal{K}} (\alpha_n^k)^* R_{n,D}^k.$
2) $(\beta_n)^* = 0$, if $\sum_{k \in \mathcal{K}} (\alpha_n^{k,t})^* R_{n,R}^k < \sum_{k \in \mathcal{K}} (\alpha_n^{k,t})^* R_{n,D}^k.$

Proof: See Appendix B. □

The MSMA algorithm is composed of initialization step and swap step. In the initialization step, Lemma 1 is utilized to help determining the communication modes, which can reduce the swap operations in the swap step. Then, in the swap step,

---

Algorithm 1 MC-Subchannel Matching Algorithm (MSMA)

Input q_U, P_U, P_M
Output β, A
Initialize β^0, A^0
repeat
  for *every subchannel* $k \in \mathcal{K}$ **do**
    while *true* **do**
      The BS searches $\mathcal{K}\backslash\{k\}$ for k' such that swap matching $\Psi_k^{k'}$ is approved, and the swap operation involving (k, k') as well as $(\Psi(k), \Psi(k'))$ is never executed in the current round;
      if *any k' is found* **then**
        Update Ψ with the found approved swap matching $\Psi_k^{k'}$;
      else
        Break;
      end
    end
  end
until *no swap operation is performed in the current iteration*;

---

we keep searching for approved swap matching.[4] The details of MSMA is provided in Algorithm 1.

B. Trajectory Optimization

Problem (37) is still non-convex due to the non-concave objective function and non-convex constraints (35f) and (35h). To tackle it efficiently, we further decompose it into two subproblems, i.e., horizontal position and altitude optimization subproblems, and then propose a trajectory optimization algorithm (TO) to solve problem (37), where the two subproblems are solved iteratively. In the following, we will first solve the two subproblems and then elaborate on the TO algorithm.

1) Horizontal Position Optimization: Given the altitude z_U, the horizontal position optimization subproblem is given by

$$\max_{x_U, y_U} \sum_{n \in \mathcal{N}} w_n R_n,$$
$$s.t. \ \|q_U - q_0\| \leq d_{max},$$
$$(35f) \text{ and } (35h). \tag{44}$$

which is still non-convex due to constraints (35h), (35f), and the non-concave objective function. To solve this problem efficiently, we can apply SCP, which will be described in detail in the following.

In iteration j, in order to find convex approximations for the non-convex functions, we first introduce concave approximations for the channel gains $h_{U,B}^k$ and $h_{n,U}^k$. Specifically, $h_{U,B}^k$ can be approximated as

$$H_{U,B}^k = |g_{U,B}^k|^2 \left(\frac{2}{L^k(x_U^{j-1}, y_U^{j-1})} - \frac{1}{\left(L^k(x_U^{j-1}, y_U^{j-1})\right)^2} L^k \right), \tag{45}$$

---

[4]The MSMA algorithm is performed by the BS. After obtaining the positions of the UEs, the BS performs the matching algorithm.

where $L^k = \overline{PR_{LoS}}PL^k_{LoS} + (1 - \overline{PR_{LoS}})PL^k_{NLoS}$, $\overline{PR_{LoS}} = \frac{2}{D^{j-1}} - \frac{1}{(D^{j-1})^2} - \frac{a}{(D^{j-1})^2}\exp\left(-b(\overline{\theta} - a)\right)$, $D^{j-1} = 1 + a\exp\left(-b\left(\overline{\theta}(x^{j-1}_U, y^{j-1}_U) - a\right)\right)$, $\overline{\theta} = \frac{180}{\pi}\left(\sin^{-1}(\frac{1}{C^{j-1}}) + (\frac{-1}{C^{j-1}\sqrt{(C^{j-1})^2-1}})(\frac{d_{U,B}}{z_U-H_B} - C^{j-1})\right)$, and $C^{j-1} = \frac{d_{U,B}(x^{j-1}_U, y^{j-1}_U)}{z_U - H_B}$. Also, $H^k_{n,U}$, the approximation for $h^k_{n,U}$, is defined as

$$H^k_{n,U} = |g^k_{U,n}|^2\left(\frac{2}{M^k_n(x^{j-1}_U, y^{j-1}_U)} - \frac{1}{(M^k_n(x^{j-1}_U, y^{j-1}_U))^2}M^k_n\right),$$

(46)

where $M^k_n = \overline{PR_{LoS}}PL^k_{LoS} + (1 - \overline{PR_{LoS}})PL^k_{NLoS}$, $\overline{PR^n_{LoS}} = \frac{2}{B^{j-1}_n} - \frac{1}{(B^{j-1}_n)^2} - \frac{a}{(B^{j-1}_n)^2}\exp\left(-b(\overline{\theta}_n - a)\right)$, $B^{j-1}_n = 1 + a\exp\left(-b\left(\overline{\theta}_n(x^{j-1}_U, y^{j-1}_U) - a\right)\right)$, $\overline{\theta}_n = \frac{180}{\pi}\left(\sin^{-1}(\frac{1}{A^{j-1}_n}) + (\frac{-1}{A^{j-1}_n\sqrt{(A^{j-1}_n)^2-1}})(\frac{d_{n,U}}{z_U} - A^{j-1}_n)\right)$, and $A^{j-1}_n = \frac{d_{n,U}(x^{j-1}_U, y^{j-1}_U)}{z_U}$. Then, we have the following theorem:

Theorem 1: $H^k_{U,B}$ and $H^k_{n,U}$ *are concave lower bounds for* $h^k_{U,B}$ *and* $h^k_{n,U}$, *respectively.*

Proof: The Proof is shown in Appendix C. $\square$

Using the above approximations, we can mitigate the non-convexity of constraints (35h) brought by the channel gains, i.e.,

$$\frac{P^k_n H^k_{n,U}}{\sigma^2} \geq \alpha^k_n\beta_n\gamma^{th}_1, \quad \frac{P^k_U H^k_{U,B}}{\sigma^2 + |I^k_B|^2} \geq \alpha^k_n\beta_n\gamma^{th}_2. \quad (47)$$

Besides, we can also transform the objective function of problem (44) into a concave one with the approximations $H^k_{U,B}$ and $H^k_{n,U}$, where the main idea is to find a concave approximation for $R^{k,t}_{n,R}$. The transformation process contains three steps:

Step 1: Replace $h^k_{n,U}$ and $h^k_{U,B}$ with $H^k_{n,U}$ and $H^k_{U,B}$, respectively. As a result, $R^k_{n,R}$ becomes the difference of two concave functions (DC), i.e., $\hat{J}^k_n$ and $\hat{I}^k_n$, where

$$\hat{J}^k_n = \frac{1}{2}\left(\log(P^k_n H^k_{n,U} + \sigma^2)\right.$$
$$\left. + \log(P^k_U H^k_{U,B} + (\frac{|I^k_B|^2}{\sigma^2} + 1)\sigma^2)\right),$$

$$\hat{I}^k_n = \frac{1}{2}\log\left(\sigma^2(P^k_n H^k_{n,U} + (1 + \frac{|I^k_B|^2}{\sigma^2})P^k_U H^k_{U,B}\right.$$
$$\left. + (1 + \frac{|I^k_B|^2}{\sigma^2})\sigma^2)\right). \quad (48)$$

Step 2: Approximate $\hat{I}^k_n$ by its first-order Taylor expansion. Then, we can obtain a concave approximation for $R^k_{n,R}$, which is given by

$$\hat{R}^k_{n,R} = \hat{J}^k_n - \boldsymbol{Ta}(\hat{I}^k_n), \quad (49)$$

where $\boldsymbol{Ta}(.)$ represents the first-order Taylor expansion at a given point (x^{j-1}_U, y^{j-1}_U) with respect to (x_U, y_U).

Step 3: Replace $R^k_{n,R}$ in the expression of objective function with $\hat{R}^k_{n,R}$, and the objective function is transformed into a concave function.

To ensure the convexity of the energy constraint (35f), we find an upper bound for the power consumption in the present time slot as follows,

$$P_f \leq P_0(1 + \frac{3v^2}{U^2_{tip}}) + P_i + \frac{1}{2}d_0\rho sAv^3 \triangleq P_u, \quad (50)$$

and the energy consumption constraint can be replaced with,

$$P_u\Delta T \leq E_{max}, \quad (51)$$

which is a convex constraint.

Therefore, the convex optimization subproblem for iteration j can be written as,

$$\max_{x_U, y_U} \sum_{n\in\mathcal{N}}\left(w_n\sum_{k\in\mathcal{K}}\left(\alpha^k_n\beta_n\hat{R}^k_{n,R} + \alpha^k_n(1-\beta_n)R^k_{n,D}\right)\right),$$
$$s.t. \text{ (47), and (51)},$$
$$\|\boldsymbol{q}_U - \boldsymbol{q}_0\| \leq d_{max}, \quad (52)$$

which can be solved by standard convex optimization tools [26].

2) Altitude Optimization: Given the horizontal position, the altitude optimization subproblem is given by

$$\max_{z_U} \sum_{n\in\mathcal{N}} w_n R_n$$
$$s.t. \text{ (35e), (35f), and (35h)}. \quad (53)$$

Assume that the maximum moving distance d_{max} is much smaller than the altitude of the UAV relay, and we have the following theorem

Theorem 2: Suppose z_U is feasible for problem (53). PR_{LoS} in $h^k_{U,B}$ can be approximated by a linear function, i.e,

$$PR_{LoS} = E + F\frac{z_U - z_0}{d^t_{U,B}(z_0)} \triangleq \mathbb{PR}_{LoS}, \quad (54)$$

where $F = PR_{NLoS}(z_0)PR_{LoS}(z_0)\frac{\frac{180}{\pi}b}{\sqrt{1-\sin^2(\frac{\pi}{180}\theta^t(z_0))}}$ and $E = PR_{LoS}(z_0)$. Besides, PR^n_{LoS} can be approximated by a linear function as well, i.e.,

$$PR^n_{LoS} = S_n + N_n\frac{z_U - z_0}{d_{n,U}(z_0)} \triangleq \mathbb{PR}^n_{LoS}, \quad (55)$$

where $N_n = PR^n_{NLoS}(z_0)PR^n_{LoS}(z_0)\frac{\frac{180}{\pi}b}{\sqrt{1-\sin^2(\frac{\pi}{180}\theta_n(z_0))}}$ and $S_n = PR^n_{LoS}(z_0)$.

Proof: See Appendix D. $\square$

Besides, based on the assumption, when z_U is a feasible point for problem (53), the distance $d_{n,U}$ and $d_{U,B}$ can be approximated by $d_{n,U}(z_0)$ and $d_{U,B}(z_0)$, respectively. Therefore, we have

$$h^k_{U,B} \approx |g^k_{U,B}|^2\Big/\left(\mathbb{PR}_{LoS}L^k(d_{U,B}(z_0))^2\eta_{LoS}\right.$$
$$\left. + (1 - \mathbb{PR}_{LoS})L^k(d_{U,B}(z_0))^2\eta_{NLoS}\right) \triangleq (h^k_{U,B})', \quad (56)$$

$$h^k_{n,U} \approx |g^k_{U,n}|^2\Big/\left(\mathbb{PR}^n_{LoS}L^k(d_{n,U}(z_0))^2\eta_{LoS}\right.$$
$$\left. + (1 - \mathbb{PR}^n_{LoS})L^k(d_{n,U}(z_0))^2\eta_{NLoS}\right) \triangleq (h^k_{n,U})', \quad (57)$$

Algorithm 2 TO Algorithm

Input $\boldsymbol{A}$, $\boldsymbol{\beta}$, $\boldsymbol{P_U}$, $\boldsymbol{P_M}$.
Output $\boldsymbol{q_U}$.
Initialize $\boldsymbol{q_U}^0$, $s = 1$.
repeat
 Solve problem (44) given z_U^{s-1}, and denote the
 solution as (x_U^s, y_U^s).
 Solve problem (53) given (x_U^s, y_U^s), and denote the
 solution as z_U^s.
 Update $s = s + 1$.
until *The fractional increase of the objective value is
below the pre-determined threshold $\epsilon_{TO} > 0$.;*

Algorithm 3 JMS-T-P Algorithm

Initialize $\boldsymbol{P_U}^0, \boldsymbol{P_M}^0, \boldsymbol{q_U}^0$; *Let $r = 1$.*
repeat
 Solve problem (36) given $\{\boldsymbol{P_U}^{r-1}, \boldsymbol{P_M}^{r-1}, \boldsymbol{q_U}^{r-1}\}$,
 and denote the solution as $(\boldsymbol{\beta}^r, \boldsymbol{A}^r)$.
 Solve problem (37) given $\{\boldsymbol{\beta}^r, \boldsymbol{A}^r, \boldsymbol{P_U}^{r-1}, \boldsymbol{P_M}^{r-1}\}$,
 and denote the solution as $\boldsymbol{q_U}^r$.
 Solve problem (38) given $\{\boldsymbol{\beta}^r, \boldsymbol{A}^r, \boldsymbol{q_U}^r\}$, and denote
 the solution as $(\boldsymbol{P_U}^r, \boldsymbol{P_M}^r)$.
 Update $r = r + 1$.
until *The increase of the objective value is below the
pre-determined threshold $\epsilon > 0$;*

---

where $(h_{U,B}^k)'$ and $(h_{n,U}^k)'$ can be found to be convex. Thus, we can use SCP method to solve problem (53). Specifically, in the l-th iteration, we first obtain concave lower bounds of $(h_{U,B}^k)'$ and $(h_{n,U}^k)'$ by applying the first-order Taylor expansions at $(z_U)^{l-1}$. Then, convex constraints and a lower bound for the objective function can be obtained by the steps introduced in Section IV-B.1. Besides, constraint (35f) can also be replaced with the constraint (51), which is convex with respect to UAV altitude z_U.

Based on the above two subsections, TO algorithm is proposed to solve the trajectory optimization problem (37). In iteration s of TO algorithm, we first optimize the horizontal position. Afterwards, given the horizontal position result, the altitude is optimized. The algorithm is summarized in Algorithm 2.

C. Power Allocation

In this subsection, we optimize the power allocation by solving problem (38). For problem (38), the constraints are convex while the objective function is non-concave. We also use the SCP method to solve this problem. For iteration o, we first transform the objective function of power allocation problem (38) into a concave one, and then solve the modified power allocation problem, which will be described in detail in the following. Note that R_n is a DC, i.e., $R_n = K_n - M_n$, where

$$K_n = \sum_{k \in \mathcal{K}} \frac{1}{2} \beta_n \alpha_n^k \log_2$$

$$\times \left((P_n^k h_{n,U}^k + \sigma^2)(P_U^k h_{U,B}^k + (\frac{|I_B^k|^2}{\sigma^2} + 1)\sigma^2) \right)$$

$$+ \sum_{k \in \mathcal{K}} (1 - \beta_n)\alpha_n^k R_{n,D}^k, \tag{58}$$

$$M_n = \sum_{k \in \mathcal{K}} \frac{1}{2} \beta_n \alpha_n^k \log_2 \left(\sigma^2 (P_n^k h_{n,U}^k + (1 + \frac{|I_B^k|^2}{\sigma^2}) P_U^k h_{U,B}^k \right.$$

$$\left. + (1 + \frac{|I_B^k|^2}{\sigma^2})\sigma^2) \right). \tag{59}$$

Therefore, by replacing M_n with its first-order Taylor expansion, we can obtain a concave approximation for R_n, i.e., $K_n - \boldsymbol{Tp}(M_n)$, where $\boldsymbol{Tp}(.)$ represents the first-order Taylor expansion at $(\boldsymbol{P_U}^{o-1}, \boldsymbol{P_M}^{o-1})$. Therefore, the power

allocation problem can be transformed into

$$\max_{\boldsymbol{P_U}, \boldsymbol{P_M}} \sum_{n \in \mathcal{N}} w_n \left(K_n - \boldsymbol{Tp}(M_n) \right) \tag{60a}$$

$$s.t. \text{ (35b), (35c), (35g), and (35h)}, \tag{60b}$$

which is convex since the non-concavity of the objective function has been eliminated.

D. Overall Algorithm

Based on the above three subsections, we propose algorithm JMS-T-P for problem (35). Specifically, in each iteration, we first optimize the communication mode $\boldsymbol{\beta}$ and subchannel allocation $\boldsymbol{A}$ by solving problem (36), given the transmit power $(\boldsymbol{P_U}, \boldsymbol{P_M})$ and trajectory $\boldsymbol{q_U}$. Then, given the communication mode $\boldsymbol{\beta}$, subchannel allocation $\boldsymbol{A}$, and transmit power $(\boldsymbol{P_U}, \boldsymbol{P_M})$, the trajectory of UAV $\boldsymbol{q_U}$ is optimized by solving problem (37). Finally, transmit power $(\boldsymbol{P_U}, \boldsymbol{P_M})$ is optimized by solving problem (38), given communication mode $\boldsymbol{\beta}$, subchannel allocation $\boldsymbol{A}$ and trajectory $\boldsymbol{q_U}$. The JMS-T-P algorithm is summarized in Algorithm 3.[5]

V. OVERALL CONVERGENCE AND COMPLEXITY ANALYSIS

In this section, we first discuss the convergence of algorithm MSMA and JMS-T-P. Then, we provide the complexity of MSMA. Finally, some results on the system performance are given.

A. Convergence Analysis

Proposition 1: MSMA converges after a limited number of swap operations.

Proof: Given swap operation l, we define the matchings before and after swap operation l by Ψ_{l-1} and Ψ_l, respectively. Besides, it is assumed that the pair of subchannels and their matches involved in this swap operation are (k_1, k_2) and (n_1, n_2), respectively, where $n_1 = \Psi_{l-1}(k_1)$ and $n_2 = \Psi_{l-1}(k_2)$. According to the definition of approved swap matching, after swap operation l, the utilities of UE n_1 and n_2 do not decrease and at least one of them increases.

---

[5]When applying SCP, the transmit power or the UAV trajectory is initialized with its most recently updated value.

Besides, for any other UE, its matching under Ψ_l is the same as that under Ψ_{l-1}, and thus, its utility remains unchanged. Therefore, the total utility of the system strictly increases after one swap operation, which implies the matching after a swap operation is different from any matching generated before. Note that the number of matchings is limited. Therefore, we can conclude that MSMA converges after a limited number of swap operations. □

Proposition 2: The JMS-T-P algorithm is guaranteed to converge.

Proof: For simplicity of discussion, we define $g(\boldsymbol{\beta}, \boldsymbol{A}, \boldsymbol{P_U}, \boldsymbol{P_M}, \boldsymbol{q_U}) = \sum_{n \in \mathcal{N}} w_n R_n$. First, in iteration r of JMS-T-P, the mode selection and subchannel allocation subproblem (36) is solved given $\{\boldsymbol{P_U}^{r-1}, \boldsymbol{P_M}^{r-1}, \boldsymbol{q_U}^{r-1}\}$. Therefore, we have

$$g(\boldsymbol{\beta}^r, \boldsymbol{A}^r, \boldsymbol{P_U}^{r-1}, \boldsymbol{P_M}^{r-1}, \boldsymbol{q_U}^{r-1})$$
$$\geq g(\boldsymbol{\beta}^{r-1}, \boldsymbol{A}^{r-1}, \boldsymbol{P_U}^{r-1}, \boldsymbol{P_M}^{r-1}, \boldsymbol{q_U}^{r-1}). \quad (61)$$

Then, we optimize the trajectory of the UAV relay, given $(\boldsymbol{\beta}^r, \boldsymbol{A}^r, \boldsymbol{P_U}^{r-1}, \boldsymbol{P_M}^{r-1})$. Thus, we can obtain the following inequality

$$g(\boldsymbol{\beta}^r, \boldsymbol{A}^r, \boldsymbol{P_U}^{r-1}, \boldsymbol{P_M}^{r-1}, \boldsymbol{q_U}^r)$$
$$\geq g(\boldsymbol{\beta}^r, \boldsymbol{A}^r, \boldsymbol{P_U}^{r-1}, \boldsymbol{P_M}^{r-1}, \boldsymbol{q_U}^{r-1}). \quad (62)$$

Afterwards, the power allocation $(\boldsymbol{P_U}, \boldsymbol{P_M})$ is optimized, given $(\boldsymbol{\beta}^r, \boldsymbol{A}^r, \boldsymbol{q_U}^r)$. As a result, we have

$$g(\boldsymbol{\beta}^r, \boldsymbol{A}^r, \boldsymbol{P_U}^r, \boldsymbol{P_M}^r, \boldsymbol{q_U}^r)$$
$$\geq g(\boldsymbol{\beta}^r, \boldsymbol{A}^r, \boldsymbol{P_U}^{r-1}, \boldsymbol{P_M}^{r-1}, \boldsymbol{q_U}^r). \quad (63)$$

Based on (61), (62) and (63), we can conclude that

$$g(\boldsymbol{\beta}^r, \boldsymbol{A}^r, \boldsymbol{P_U}^r, \boldsymbol{P_M}^r, \boldsymbol{q_U}^r)$$
$$\geq g(\boldsymbol{\beta}^{r-1}, \boldsymbol{A}^{r-1}, \boldsymbol{P_U}^{r-1}, \boldsymbol{P_M}^{r-1}, \boldsymbol{q_U}^{r-1}), \quad (64)$$

which means that the objective value of problem (35) is non-decreasing after each iteration of JMS-T-P algorithm. Besides, since the radio resource in the network is limited, there is an upper bound for the data rate of each UE. Thus, the objective value of problem (35) is upper bounded. Therefore, JMS-T-P is guaranteed to converge [20]. □

B. Complexity Analysis

Proposition 3: In each iteration of MSMA, at most $\frac{1}{2}K(K-1)(N-1)$ swap matchings need to be considered. Given the number of iterations I, the complexity of MSMA is $O(INK^2)$

Proof: Suppose subchannel k_1 is matched. For k_1, $N-1$ UE pairs (n_1, n_2) satisfying that n_1 is matched with k_1 and n_2 is not matched with k_1 can be found, because each subchannel is assigned to at most one UE and the number of UEs is N. For n_2, at most $K-1$ subchannels are matched with it. Therefore, a swap matching $\Psi_{k_1}^{k_2}$ with k_1 fixed has at most $(N-1)(K-1)$ combinations. Since the maximum number of matched subchannel is K, at most $\frac{1}{2}K(K-1)(N-1)$ swap matchings should be considered. Therefore, given number of iterations I, the complexity of MSMA is $O(INK^2)$. □

C. System Performance Analysis

In the following proposition, we will discuss the trend of the average UAV speed when the maximum velocity of the UAV changes.

Proposition 4: When maximum velocity v_{max} of the UAV increases, the average speed of the UAV becomes larger first, and then converges.

Proof: We first show that when v_{max} is small, the average speed of the UAV is positively correlated with v_{max}. To satisfy the QoS requirement, the UAV has to fly to different locations when serving different UEs. Define l_{avg} as the average distance that the UAV flies when it turns to serve another UE. The average speed of the UAV relay can thus be expressed as $\frac{N_r l_{avg}}{T D_T}$, where N_r is the number of UEs served by the UAV relay, and D_T is the length of each time slot. Since the UE locations, number of time slots T, and slot length D_T are given, we will focus on the influence of v_{max} on N_r in the following.

To derive the expression of N_r, we first model the relationship between the sum of logarithmic data rate and N_r. The number of time slots that the UAV relay spends on changing locations to serve different UEs can be calculated as $T_f = \frac{N_r l_{avg}}{v_f D_T}$, where v_f is the average velocity of the UAV when it flies to serve another UE. Therefore, one UE in the relay mode can occupy $\frac{T - T_f}{N_r}$ time slots on average to transmit signals to the BS. Note that when v_f increases, the time spent on flying can be reduced, and thus, each UE in the relay mode has more time to transmit. Therefore, v_f should be maximized. According to the expression of the flying power consumption, i.e.,

$$P_f(v) = P_0(1 + \frac{3v^2}{U_{tip}^2}) + P_i(\sqrt{1 + \frac{v^4}{4v_0^4}} - \frac{v^2}{2v_0^2})^{\frac{1}{2}} + \frac{d_0 \rho s A v^3}{2}, \quad (65)$$

the flying power increases with the UAV speed on the whole. Therefore, the battery capacity constraint can be neglected for now since v_{max} is small. As a result, v_f can be maximized as v_{max}. Denote the instantaneous data rate of one UE in the relay mode by R_r. The average data rate of such a UE can thus be given by $R_r \frac{T - T_f}{N_r} \frac{1}{T}$. Therefore, the sum of logarithmic data rate over all UEs can be expressed as

$$\sum_{n \in \mathcal{N}} R_n^{avg} = N_c \log_2(R_{avg}^c) + N_r \log_2(R_r \frac{T - T_f}{N_r T}), \quad (66)$$

where N_c is the number of UEs in the cellular mode, and R_{avg}^c is the average rate of one UE in the cellular mode. Then, we obtain the optimal N_r based on the expression of the sum logarithmic rate. Specifically, we first formulate a function $f(x) = N_c \log_2(R_{avg}^c) + x \log_2(R_r \frac{T - T_f}{xT})$. By analyzing its derivative, we can find that f is monotonically decreasing in $[0, \frac{R_r}{x_0 + c})$, and increasing in $[\frac{R_r}{x_0 + c}, \infty)$, where x_0 is the zero point of the function $g(x) = \frac{2}{-\ln 2} - \frac{c}{\ln 2} x^{-1} + \log_2 x$, and $c = \frac{R_r l_{avg}}{T v_{max}}$. Therefore, the optimal number of UEs served by the UAV relay can be approximated as

$$N_r = \lfloor \frac{R_r}{x_0 + c} \rfloor. \quad (67)$$

It can be found that when v_{max} increases, c becomes smaller. Note that g is monotonically increasing, and $g(x)$ is negatively correlated with c when x is given. Therefore, zero point x_0 decreases with v_{max}, and thus, N_r increases with v_{max}. As a result, we can conclude that the average UAV speed is positively correlated with maximum speed v_{max}.

Then, we show that when v_{max} is large, the average speed will converge. Since the number of UEs in the relay mode is limited by N, the average speed cannot exceed $\frac{N l_{avg}}{T D_T}$. Besides, due to the flying energy constraint, the flying power consumption in each time slot is smaller than E_u, and thus, the velocity of the UAV in each time slot is limited. Therefore, when v_{max} is large, the average speed will converge. $\square$

Consider any two disjoint regions within the cell coverage, denoted by $\mathcal{A}$ and $\mathcal{B}$, respectively. The numbers of UEs within region $\mathcal{A}$ and in $\mathcal{B}$ are represented by N_A and N_B, respectively, satisfying $N_A \geq N_B$. Define T_A and T_B as the time period that the UAV spends within region $\mathcal{A}$, and $\mathcal{B}$, respectively. In the following, we consider the influence of UE numbers N_A and N_B on flight time T_A and T_B.

Proposition 5: The UAV spends more time within regions with more UEs, i.e., $T_A \geq T_B$. Besides, when N_A or N_B is given, $\frac{T_B}{T_A}$ increases with $\frac{N_B}{N_A}$.

Proof: Denote the instantaneous data rate of one UE within region s by R_s, where $s \in \{\mathcal{A}, \mathcal{B}\}$. To prove the proposition, we first model the relationship between flight time (T_A, T_B) and the instantaneous data rate. Specifically, to maximize user fairness among the UEs within the two regions, T_A and T_B should be set such that the average rate of these UEs are the same. Since the average rate of one UE within region s can be expressed as $\frac{R_s T_s}{T}$, we have

$$\frac{R_A T_A}{T} = \frac{R_B T_B}{T}, \tag{68}$$

which can be simplified into

$$\frac{T_A}{T_B} = \frac{R_B}{R_A}. \tag{69}$$

Then, we investigate how numbers N_A and N_B of UEs affect instantaneous data rate R_A and R_B. During T_A, the UEs in the region $\mathcal{A}$ can transmit to the BS simultaneously through the UAV relay due to OFDMA. However, the UEs in the region $\mathcal{B}$ cannot transmit in the relay mode due to severe pathloss between the UAV and these UEs. Therefore, the average UAV transmit power allocated to one UE in region $\mathcal{A}$ is $\frac{P_U^{max}}{N_A}$. Similarly, during T_B, the UAV transmit power allocated to one UE in region $\mathcal{B}$ can be expressed as $\frac{P_U^{max}}{N_B}$. Since the instantaneous data rate of one UE is positively correlated with the allocated UAV transmit power, we have $R_A \leq R_B$ since $N_A \geq N_B$. Therefore, it can be found that $T_A \geq T_B$.

Then, we show that when N_s ($s \in \{\mathcal{A}, \mathcal{B}\}$) is given, $\frac{T_B}{T_A}$ increases with $\frac{N_B}{N_A}$. Without loss of generality, we assume that $s = \mathcal{B}$. When $\frac{N_B}{N_A}$ increases, number N_A of UEs decreases since N_B is given. Therefore, instantaneous data rate R_A becomes larger while R_B remains unchanged. Therefore, $\frac{T_B}{T_A}$ increases with $\frac{N_B}{N_A}$. $\square$

TABLE I
SIMULATION PARAMETERS

| Parameters	Values
Number of UEs N	5
Number of subchannels K	10
Number of time slots T	10
Duration of one time slot ΔT	1 s
Height of BS H_B	30 m
Maximum moving distance d_{max}	15 m
Maximum transmit power of the UAV relay P_U^{max}	0.3 W
SNR threshold γ^{th}	300
Pathloss exponent for terrestrial communications α	4
Noise variance σ^2	-96 dBm
Air-to-ground channel parameters η_{LoS}	1 dB
Air-to-ground channel parameters η_{NLoS}	20 dB
Air-to-ground channel parameters a	9.6
Air-to-ground channel parameters b	0.28
Frequency of subchannel k f^k	1 GHz
Stop criterion for JMS-T-P ϵ	0.001
Stop criterion for TO ϵ_{TO}	0.01
ICI power $|I_B^k|^2$	-110 dBm
Profile drag coefficient δ	0.012
Blade angular velocity Ω	300 rad/s
Rotor radius R	0.4 m
Tip speed of the rotor blade U_{tip}	120 m/s
Mean rotor induced velocity in hover v_0	4.03
Fuselage drag ratio d_0	0.6
Air density ρ	1.225 kg/m^3
Rotor solidity s	0.05
Rotor disc area A	0.503 m^2
Means aircraft weight W	20 N
Incremental correction factor to induced power k	0.1

VI. SIMULATION RESULTS

In this section, we evaluate the performance of the proposed JMS-T-P algorithm. The selection of simulation parameters is based on existing works [27]. In the simulation, the initial horizontal positions of the UAV and the UEs are uniformly distributed within a circle with the BS as center and $200\ m$ as radius. Besides, the altitude of the UAV relay z_U^1 obeys a uniform distribution between $[100\ m, 200\ m]$. Other simulation parameters are listed in Table I.

For comparison, the following algorithms are also performed:

- **Random algorithm**: We determine the communication mode and allocate subchannels randomly while the trajectory optimization and the power allocation are performed in the same way as in the JMS-T-P algorithm.
- **Cellular scheme**: All the UEs transmit in the cellular mode, and the subchannel allocation and the transmit power of the UEs are jointly optimized to maximize the weighted sum rate, i.e., $\sum_{n \in \mathcal{N}} w_n R_n$.

Fig. 2 depicts the influence of the maximum transmit power P_M^{max} on the sum rate. From Fig. 2, we can find that the sum rate is positively correlated with the maximum transmit
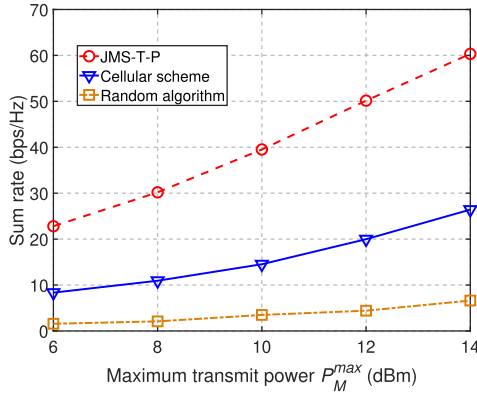
Fig. 2. Sum rate vs. maximum transmit power with $d_{max} = 25$ m.
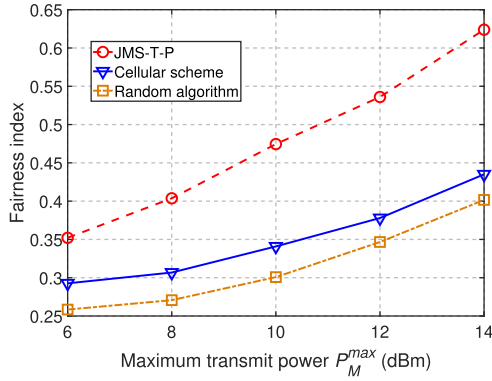
Fig. 3. Fairness vs. maximum transmit power with $d_{max} = 25$ m.

Fig. 4. Number of UEs vs. maximum transmit power with $d_{max} = 25$ m.

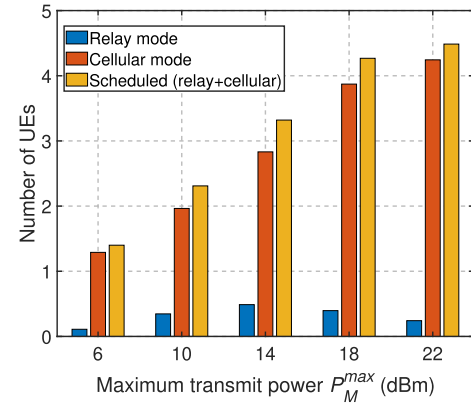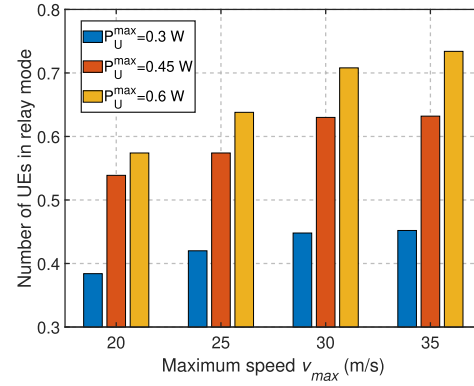Fig. 5. Number of UEs in the relay mode vs. maximum speed of the UAV relay, with $P_M^{max} = 17$ dBm.

power P_M^{max}. Besides, it can be observed that the proposed JMS-T-P algorithm always outperforms the random algorithm in terms of the sum rate, since subchannel allocation and communication modes are determined randomly in the random algorithm. Moreover, Fig. 2 shows that the JMS-T-P achieves larger sum rate than the cellular scheme, since in the cellular scheme, the UEs in the cell edge cannot transmit to the BS.

Fig. 3 depicts the fairness index versus the maximum transmit power. To evaluate the user fairness, we introduce Jain's fairness index [28] which can be calculated as

$$\frac{(\sum_{n\in\mathcal{N}} R_n^{avg})^2}{N\sum_{n\in\mathcal{N}} (R_n^{avg})^2}. \tag{70}$$

The index varies from 0 to 1, and a larger value implies a higher fairness. As indicated in Fig. 3, higher transmit power will guarantee better user fairness, since more UEs can transmit to the BS. Besides, we can also find that the JMS-T-P algorithm achieves higher fairness than the cellular scheme, since the cell edge UEs cannot transmit to the BS in the cellular scheme. Moreover, according to Fig. 3, the JMS-T-P leads to better fairness among the UEs than the random algorithm, which demonstrates the effectiveness the JMS-T-P algorithm.

Fig. 4 shows how the maximum transmit power P_M^{max} influences the transmission modes of the UEs. We can observe that as the maximum transmit power increases, the number of scheduled UEs first increases and then saturates. Note that

the SNR is positively correlated with the maximum transmit power. Therefore, when the maximum transmit power is small, more UEs will be scheduled if the maximum transmit power increases. However, the number of scheduled UEs will remain a constant when the maximum transmit power is sufficiently large since the number of UEs is fixed in this system. Besides, when the maximum transmit power is large, fewer UEs transmit in the relay mode as the maximum transmit power increases. This is because some UEs switch from the relay mode to the cellular mode.

Fig. 5 depicts the number of UEs in the relay mode versus the maximum speed of the UAV. It can be observed that when the mobility of the UAV relay strengthens, more UEs will transmit in the relay mode. This is because the UAV can spend less time flying to serve another UE, during which no UE can transmit in the relay mode. Besides, we can also find that the number of UEs in the relay mode will decrease under a lower transmit power P_U^{max}. This is because the UAV relay has to move closer to the BS in order to satisfy the QoS constraint for the UAV-BS link, and thus, some UEs previously transmitting in the relay mode cannot send data through the UAV relay now.

Fig. 6 depicts the average speed of the UAV relay versus maximum speed v_{max}. We can find that when v_{max} increases, the average speed becomes larger first, and then converges, which is consistent with Proposition 4. Moreover, it can be
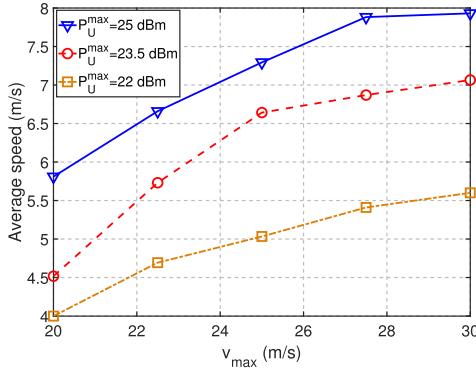
Fig. 6. Average speed vs. maximum speed of the UAV relay, with $P_M^{max} = 17$ dBm.

observed that the average speed is positively correlated with the transmit power P_U^{max}. This is because there are more UEs which can transmit in the relay mode if the UAV relay flies to proper locations, and thus, the UAV moves for a larger distance in order to serve these additional UEs.

VII. CONCLUSION

In this paper, we have studied a multi-user OFDMA cellular network with one UAV relay. Aiming to improve the throughput while guaranteeing the user fairness, we have formulated a series of joint mode selection, subchannel allocation, trajectory optimization and power allocation problems. Since the formulated problem is NP-hard, we have proposed the efficient JMS-T-P algorithm to obtain a suboptimal solution, where mode selection and subchannel allocation, trajectory optimization, and power allocation were performed iteratively. The simulation results have shown that JMS-T-P outperforms the random algorithm and the cellular scheme. Besides, based on the theoretical analysis, two important conclusions can be obtained. First, when maximum velocity of the UAV increases, the average speed of the UAV becomes larger first, and then converges. Second, the UAV spends more time within regions with more UEs.

APPENDIX A
APPROXIMATIONS FOR INTER-SUBCARRIER-INTERFERENCE

First, we focus on the ICI to subchannels allocated to UEs in the cellular mode. Specifically, the ICI to subchannel k can be approximated by [29]

$$I_B^k = \sum_{n' \in \mathcal{N}_R} \sum_{k' \in \mathcal{K}_{n'}} \left(\frac{\sin(\pi(f_{d,max}/\Delta f - k + k'))}{K \sin(\frac{\pi(f_{d,max}/\Delta f - k + k')}{K})} \right.$$
$$\left. \times e^{j\pi(f_{d,max}/\Delta f - k + k')\frac{K-1}{K}} \sqrt{\frac{P_{n'}^{k'} G^{k'} K}{PL_{avg}^c}} h_{n',U}^{k'} X_{n'}^{k'} \right),$$
(71)

where $\mathcal{N}_R$ is the set of UEs in the relay mode, $\mathcal{K}_{n'}$ represents the set of subcarriers allocated to UE n', K denotes the total number of subcarriers in the system, $f_{d,max}$ is maximum Doppler shift, Δf denotes the subcarrier spacing, PL_{avg}^c

represents the average pathloss from the UAV to the BS over the center frequency, $G^{k'}$ is the amplification coefficient of the UAV relay over subchannel k', and $X_{n'}^{k'}$ denotes the data symbol transmitted by UE $n' \in \mathcal{N}_R$ over subchannel k' with unit power. Here, the maximum Doppler shift can be given by $f_{d,max} = \frac{vf_c}{c}$, where v is the velocity of the UAV, f_c represents the center frequency, and c is the velocity of light in vacuum. By setting the parameters to their typical values [27], [30], the ratio of the ICI power to the desired signal power can be calculated to be -16.1 dB, which indicates that the ICI is weak compared with the desired signal. Here, the number of subchannels are set as $K = 1000$, the subcarrier spacing is $\Delta f = 15$ KHz, the center frequency is $f_c = 3.5$ GHz, the UAV speed is $v = 100$ km/h, and the pathloss ratio is set to be $\eta = 15$ dB.

Then, we turn to the transmission in the relay mode, where an approximation for the ICI over subchannel k is given below [29],

$$I_B^k = \sum_{n' \in \mathcal{N}_R, n' \neq n} \sum_{k' \in \mathcal{K}_{n'}} \left(\frac{\sin(\pi(\epsilon - k + k'))}{K \sin(\frac{\pi(f_{d,max}/\Delta f - k + k')}{K})} \right.$$
$$\left. \times e^{j\pi(f_{d,max}/\Delta f - k + k')\frac{K-1}{K}} \sqrt{\frac{P_{n'}^{k'} G^{k'} K}{PL_{avg}^c}} h_{n',U}^{k'} X_{n'}^{k'} \right)$$
$$+ \sum_{k' \in \mathcal{K}_n, k' \neq k} \left(\frac{\sin(\pi(f_{d,max}/\Delta f - k + k'))}{K \sin(\frac{\pi(f_{d,max}/\Delta f - k + k')}{K})} \right.$$
$$\left. \times e^{j\pi(f_{d,max}/\Delta f - k + k')\frac{K-1}{K}} \sqrt{\frac{P_n^{k'} G^{k'} K}{PL_{avg}^c}} h_{n,U}^{k'} X_n^{k'} \right).$$
(72)

Under the parameter settings, the ICI power can be found to be -31.1 dB lower than the desired signal power.

APPENDIX B
PROOF OF LEMMA 1

We prove the first statement first. From $\sum_{k \in \mathcal{K}} (\alpha_n^k)^* R_{n,R}^k > \sum_{k \in \mathcal{K}} (\alpha_n^k)^* R_{n,D}^k$, we can infer that if UE n adopts the relay mode, its average transmission rate R_n^{avg} is larger than that when the cellular mode is adopted. Note that the communication mode β_n will only affect R_n, which has a positive influence on weighted sum rate $\sum_{n \in \mathcal{N}} w_n R_n$. Therefore, sum rate $\sum_{n \in \mathcal{N}} w_n R_n$ under the relay mode is larger than that under the cellular mode. Besides, according to (42) and (43), when UE n transmits in either of the communication modes, the SNR requirements are satisfied. Thus, UE n will adopt the relay mode, i.e., $(\beta_n)^* = 1$. Similarly, we can prove the second statement, and thus the proof is neglected here.

APPENDIX C
PROOF OF THEOREM 1

First, we prove that $H_{U,B}^k$ is a lower bound for $h_{U,B}^k$. It can be observed that the elevation angle θ in the formulation of $h_{U,B}^k$ is convex with respect to $\frac{d_{U,B}}{z_U - H_B}$. Recall that any convex function is globally lower-bounded by its first-order Taylor

expansion at any point. Therefore, with point C^{j-1}, we have

$$\theta \geq \frac{180}{\pi}\left(\sin^{-1}(\frac{1}{C^{j-1}}) + \frac{C^{j-1} - \frac{d_{U,B}}{z_U^t - H_B}}{C^{j-1}\sqrt{(C^{j-1})^2 - 1}}\right) = \overline{\theta}. \quad (73)$$

Then, the probability of LoS connection from the UAV to the BS is lower bounded by,

$$PR_{LoS} \geq \frac{1}{1 + a\exp\left(-b(\overline{\theta} - a)\right)} \quad (74)$$

Since $[1 + a\exp\left(-b(\overline{\theta} - a)\right)]$ always takes positive values, the right-hand-side (RHS) of (74) is convex with respect to it. Therefore, with point D^{j-1}, we have

$$\frac{1}{1 + a\exp\left(-b(\overline{\theta} - a)\right)} \geq \frac{2}{D^{j-1}} - \frac{1}{(D^{j-1})^2} - \frac{a}{(D^{j-1})^2}$$
$$\times \exp\left(-b(\overline{\theta} - a)\right)$$
$$= \overline{PR_{LoS}}, \quad (75)$$

which means $\overline{PR_{LoS}}$ is also a lower bound for PR_{LoS}. Then, by replacing PR_{LoS} in the expression of $h_{U,B}^k$ with $\overline{PR_{LoS}}$, $h_{U,B}^k$ is lower bounded by

$$h_{U,B}^k \geq \frac{1}{(d_{U,B})^2\left(L^k\eta_{NLoS} + (L^k\eta_{LoS} - L^k\eta_{NLoS})\overline{PR_{LoS}}\right)}$$
$$= \frac{1}{L^k}. \quad (76)$$

Note that $\frac{1}{L^k}$ is convex with respect to L^k. Therefore, with point $L^k(x_U^{j-1}, y_U^{j-1})$, we have

$$\frac{1}{L^k} \geq \frac{2}{L^k(x_U^{j-1}, y_U^{j-1})} - \frac{1}{(L^k(x_U^{j-1}, y_U^{j-1}))^2}L^k = H_{U,B}^k. \quad (77)$$

Based on (76) and (77), we can conclude that $H_{U,B}^k$ is a lower bound for $h_{U,B}^k$. Then, we show the concavity of $H_{U,B}^k$. It can be proved that L^k is convex. Therefore, according to (77), we can easily find that $H_{U,B}^k$ is a concave function with respect to (x_U, y_U).

Similarly, we can prove that $H_{n,U}^k$ is a concave lower bound for $h_{n,U}^k$, and thus the proof is neglected here.

APPENDIX D
PROOF OF THEOREM 2

First, we show that PR_{LoS} can be approximated by $\mathbb{PR}_{LoS}$. Since z_U is feasible, the maximum moving distance of the UAV relay in the present time slot is d_{max}. Besides, the altitude z_U is much larger than d_{max}. Therefore, the distance $d_{U,B}$ is approximately equal to $d_{U,B}(z_U)$, and thus the elevation angle θ in the expression of PR_{LoS} can be rewritten as $\theta \approx \frac{180}{\pi}\sin^{-1}(\frac{z_U - H_B}{d_{U,B}(z_U)} + q_s)$, where $q_s = \frac{z_U - z_U}{d_{U,B}(z_U)}$. Note that q_s is a tiny quantity. Therefore, PR_{LoS} can be approximated by its first-order Taylor expansion with respect to q_s, which is calculated to be $\mathbb{PR}_{LoS}$. Similarly, we can prove that $\mathbb{PR}_{LoS}^n$ approximates PR_{LoS}^n, and thus the proof is neglected here.

REFERENCES

[1] S. Zeng, H. Zhang, and L. Song, "Trajectory optimization and resource allocation for multi-user OFDMA UAV relay networks," in *Proc. IEEE GLOBECOM*, Waikoloa, HI, USA, Dec. 2019, pp. 1–6.

[2] X. Chen, X. Hu, Q. Zhu, W. Zhong, and B. Chen, "Channel modeling and performance analysis for UAV relay systems," *China Commun.*, vol. 15, no. 12, pp. 89–97, Dec. 2018.

[3] S. Zeng, H. Zhang, K. Bian, and L. Song, "UAV relaying: Power allocation and trajectory optimization using decode-and-forward protocol," in *Proc. IEEE ICC Workshops*, Kansas City, MO, USA, May 2018, pp. 1–6.

[4] A. Merwaday and I. Guvenc, "UAV assisted heterogeneous networks for public safety communications," in *Proc. IEEE WCNCW*, New Orleans, LA, USA, Mar. 2015, pp. 329–334.

[5] R. Grodi, D. B. Rawat, and C. Bajracharya, "Performance evaluation of unmanned aerial vehicle ad hoc networks," in *Proc. SoutheastCon*, Fort Lauderdale, FL, USA, Apr. 2015, pp. 1–4.

[6] X. Zhong, Y. Guo, N. Li, and S. Li, "Deployment optimization of UAV relays for collecting data from sensors: A potential game approach," *IEEE Access*, vol. 7, pp. 182962–182973, Dec. 2019.

[7] S. Zhang, H. Zhang, Q. He, K. Bian, and L. Song, "Joint trajectory and power optimization for UAV relay networks," *IEEE Commun. Lett.*, vol. 22, no. 1, pp. 161–164, Jan. 2018.

[8] K. Li, W. Ni, X. Wang, R. P. Liu, S. S. Kanhere, and S. Jha, "Energy-efficient cooperative relaying for unmanned aerial vehicles," *IEEE Trans. Mobile Comput.*, vol. 15, no. 6, pp. 1377–1386, Jun. 2016.

[9] M. Bliss and N. Michelusi, "Trajectory optimization for rotary-wing UAVs in wireless networks with random requests," in *Proc. IEEE GLOBECOM*, Waikoloa, HI, USA, Dec. 2019, pp. 1–6.

[10] Y. Sun, D. Xu, D. W. K. Ng, L. Dai, and R. Schober, "Optimal 3D-trajectory design and resource allocation for solar-powered UAV communication systems," *IEEE Trans. Commun.*, vol. 67, no. 6, pp. 4281–4298, Jun. 2019.

[11] R. Li *et al.*, "Joint trajectory and resource allocation design for UAV communication systems," in *Proc. IEEE Globecom Workshops (GC Wkshps)*, Abu Dhabi, United Arab Emirates, Dec. 2018, pp. 1–6.

[12] J. Joung and S. Sun, "Power efficient resource allocation for downlink OFDMA relay cellular networks," *IEEE Trans. Signal Process.*, vol. 60, no. 5, pp. 2447–2459, May 2012.

[13] M. Köppe, "On the complexity of nonlinear mixed-integer optimization," 2010, *arXiv:1006.4895*. [Online]. Available: http://arxiv.org/abs/1006.4895

[14] Z. Liu, H. Yuan, H. Li, X. Guan, and H. Yang, "Robust power control for amplify-and-forward relaying scheme," *IEEE Commun. Lett.*, vol. 19, no. 2, pp. 263–266, Feb. 2015.

[15] C. Di Franco and G. Buttazzo, "Energy-aware coverage path planning of UAVs," in *Proc. IEEE Int. Conf. Auton. Robot Syst. Competitions*, Vila Real, Portugal, Apr. 2015, pp. 111–117.

[16] A. Filippone, *Flight Performance of Fixed and Rotary Wing Aircraft* (Butterworth-Heinemann). Washington, DC, USA: AIAA, 2006.

[17] *Study on Enhanced LTE Support for Aerial Vehicles*, document TR 36.777, 3GPP, Dec. 2017.

[18] M. A. Gutierrez-Estevez, R. L. G. Cavalcante, S. Stanczak, J. Zhang, and H. Zhuang, "A distributed solution for proportional fairness optimization in load coupled OFDMA networks," in *Proc. IEEE GlobalSIP*, Washington, DC, USA, Dec. 2016, pp. 550–554.

[19] H. Kim, K. Kim, Y. Han, and S. Yun, "A proportional fair scheduling for multicarrier transmission systems," in *Proc. IEEE VTC-Fall*, Los Angeles, CA, USA, Sep. 2004, pp. 409–413.

[20] H. Zhang, L. Song, and Y. J. Zhang, "Load balancing for 5G ultra-dense networks using device-to-device communications," *IEEE Trans. Wireless Commun.*, vol. 17, no. 6, pp. 4039–4050, Jun. 2018.

[21] X. Li, R. Shankaran, M. A. Orgun, G. Fang, and Y. Xu, "Resource allocation for underlay D2D communication with proportional fairness," *IEEE Trans. Veh. Technol.*, vol. 67, no. 7, pp. 6244–6258, Jul. 2018.

[22] B. Di, L. Song, and Y. Li, "Sub-channel assignment, power allocation, and user scheduling for non-orthogonal multiple access networks," *IEEE Trans. Wireless Commun.*, vol. 15, no. 11, pp. 7686–7698, Nov. 2016.

[23] A. Roth and M. Sotomayor, *Two-Sided Matching: A Study in Game-Theoretic Modeling and Analysis*. Cambridge U.K.: Cambridge Univ. Press, 1992.

[24] E. Bodine-Baron, C. Lee, A. Chong, B. Hassibi, and A. Wierman, "Peer effects and stability in matching markets," in *Proc. SAGT*, Amalfi, Italy, Oct. 2011, pp. 117–129.

[25] Q. Wu, Y. Zeng, and R. Zhang, "Joint trajectory and communication design for multi-UAV enabled wireless networks," *IEEE Trans. Wireless Commun.*, vol. 17, no. 3, pp. 2109–2121, Mar. 2018.

[26] S. Boyd and L. Vandenberghe, *Convex Optimization*. Cambridge, U.K.: Cambridge Univ. Press, 2004.

[27] S. Zhang, H. Zhang, B. Di, and L. Song, "Cellular UAV-to-X communications: Design and optimization for multi-UAV networks," *IEEE Trans. Wireless Commun.*, vol. 18, no. 2, pp. 1346–1359, Jan. 2019.

[28] R. Jain, D. Chiu, and W. Hawe, "A quantitative measure of fairness and discrimination for resource allocation in shared computer systems," Digit. Equip. Corp., Hudson, MA, USA, Tech. Rep. TR-301, Sep. 1984.

[29] P. Robertson and S. Kaiser, "The effects of Doppler spreads in OFDM(A) mobile radio systems," in *Proc. IEEE VTC-Fall*, Amsterdam, The Netherlands, Sep. 1999, pp. 329–333.

[30] *Study on Enhanced LTE Support for Aerial Vehicles*, document TR 36.777, 3GPP, Dec. 2017.

Boya Di (Member, IEEE) received the B.S. degree in electronic engineering from Peking University, China, in 2014, and the Ph.D. degree from the Department of Electronics, Peking University, in 2019. Her current research interests include edge computing, vehicular networks, non-orthogonal multiple access, and 5G wireless networks. So far she has contributed as the first author for nine journal articles and one of her journal papers is currently listed as ESI highly cited papers. She has also served as a TPC member in GLOBECOM 2016, ICCC 2017, ICC 2016, ICC 2018, and VTC 2019.

Shuhao Zeng (Graduate Student Member, IEEE) received the B.S. degree with the School of Electrical Engineering and Computer Science, Peking University, in 2018, where he is currently pursuing the Ph.D. degree. His current research interests include intelligent surfaces and unmanned aerial vehicle networks.

Hongliang Zhang (Member, IEEE) received the B.S. and Ph.D. degrees from the School of Electrical Engineering and Computer Science, Peking University, in 2014 and 2019, respectively. He was a Post-Doctoral Fellow with the Electrical and Computer Engineering Department, University of Houston, Texas, from July 2019 to July 2020. He is currently a Post-Doctoral Associate with the Department of Electrical Engineering, Princeton University, NJ, USA. His current research interests include reconfigurable intelligent surfaces, aerial access networks, and game theory. He has served as a TPC Member for many IEEE conferences, such as GLOBECOM, ICC, and WCNC. He received the Best Doctoral Thesis Award from the Chinese Institute of Electronics in 2019. He is an Exemplary Reviewer for IEEE TRANSACTIONS ON COMMUNICATIONS in 2020. He is currently an Editor for *IET Communications and Frontiers in Signal Processing*. He also serves as a Guest Editor for IEEE INTERNET OF THINGS JOURNAL (IoT-J) Special Issue on Internet of UAVs over Cellular Networks.

Lingyang Song (Fellow, IEEE) received the Ph.D. degree from the University of York, U.K., in 2007. He worked as a Research Fellow with the University of Oslo, Norway, until rejoining Philips Research UK in March 2008. In May 2009, he joined the Department of Electronics, School of Electronics Engineering and Computer Science, Peking University, where he is currently a Boya Distinguished Professor. His main research interests include wireless communication and networks, signal processing, and machine learning. He received the K.M. Stott Prize for Excellent Research at University of Oslo. He was a recipient of the IEEE Leonard G. Abraham Prize in 2016 and the IEEE Asia Pacific (AP) Young Researcher Award in 2012. He has been an IEEE Distinguished Lecturer, since 2015.